

Erbium-doped waveguide DBR and DFB laser arrays integrated within an ultra-low-loss Si₃N₄ platform

Michael Belt* and Daniel J. Blumenthal

Electrical and Computer Engineering Department, University of California, Santa Barbara California 93106, USA
*michaelbelt@ece.ucsb.edu

Abstract: Record low optical threshold power and high slope efficiency are reported for arrays of distributed Bragg reflector lasers integrated within an ultra-low-loss Si₃N₄ planar waveguide platform. Additionally, arrays of distributed feedback laser designs are presented that show improvements in pump-to-signal conversion efficiency of over two orders of magnitude beyond that found in previously published devices. Lithographically defined sidewall gratings provide the required lasing feedback for both cavity configurations. Lasing emission is shown over a wide wavelength range (1534 to 1570 nm), with output powers up to 2.1 mW and side mode suppression ratios in excess of 50 dB.

©2014 Optical Society of America

OCIS codes: (130.3120) Integrated optics devices; (140.3500) Lasers, erbium; (230.1480) Bragg reflectors.

References and links

1. J. F. Bauters, M. J. R. Heck, D. D. John, J. S. Barton, C. M. Bruinink, A. Leinse, R. G. Heideman, D. J. Blumenthal, and J. E. Bowers, "Planar waveguides with less than 0.1 dB/m propagation loss fabricated with wafer bonding," *Opt. Express* **19**(24), 24090–24101 (2011).
2. M. Belt, J. Bovington, R. Moreira, J. F. Bauters, M. J. Heck, J. S. Barton, J. E. Bowers, and D. J. Blumenthal, "Sidewall gratings in ultra-low-loss Si₃N₄ planar waveguides," *Opt. Express* **21**(1), 1181–1188 (2013).
3. M. Belt, T. Huffman, M. L. Davenport, W. Li, J. S. Barton, and D. J. Blumenthal, "Arrayed narrow linewidth erbium-doped waveguide-distributed feedback lasers on an ultra-low-loss silicon-nitride platform," *Opt. Lett.* **38**(22), 4825–4828 (2013).
4. H. Park, A. Fang, S. Kodama, and J. Bowers, "Hybrid silicon evanescent laser fabricated with a silicon waveguide and III-V offset quantum wells," *Opt. Express* **13**(23), 9460–9464 (2005).
5. S. Srinivasan, A. W. Fang, D. Liang, J. Peters, B. Kaye, and J. E. Bowers, "Design of phase-shifted hybrid silicon distributed feedback lasers," *Opt. Express* **19**(10), 9255–9261 (2011).
6. R. E. Camacho-Aguilera, Y. Cai, N. Patel, J. T. Bessette, M. Romagnoli, L. C. Kimerling, and J. Michel, "An electrically pumped germanium laser," *Opt. Express* **20**(10), 11316–11320 (2012).
7. J. Bradley, L. Agazzi, D. Geskus, F. Ay, K. Wörhoff, and M. Pollnau, "Gain bandwidth of 80 nm and 2 dB/cm peak gain in Al₂O₃:Er³⁺ optical amplifiers on silicon," *J. Opt. Soc. Am. B* **27**(2), 187–196 (2010).
8. J. Purnawirman, J. Sun, T. N. Adam, G. Leake, D. Coolbaugh, J. D. Bradley, E. S. Hosseini, and M. R. Watts, "C- and L-band erbium-doped waveguide lasers with wafer-scale silicon nitride cavities," *Opt. Lett.* **38**(11), 1760–1762 (2013).
9. F. Ay and A. Aydinli, "Comparative investigation of hydrogen bonding in silicon based PECVD grown dielectrics for optical waveguides," *Opt. Mater.* **26**(1), 33–46 (2004).
10. K. Wörhoff, J. D. B. Bradley, F. Ay, D. Geskus, T. P. Blauwendraat, and M. Pollnau, "Reliable low-cost fabrication of low-loss Al₂O₃:Er³⁺ waveguides with 5.4-dB optical gain," *IEEE J. Quantum Electron.* **45**(5), 454–461 (2009).
11. E. H. Bernhardt, "Bragg-grating-based rare-earth-ion-doped channel waveguide lasers and their applications," Ph.D. dissertation (Department of Electrical Engineering, Mathematics, and Computer Science, University of Twente, 2012).
12. G. N. van den Hoven, E. Snoeks, A. Polman, C. van Dam, J. W. M. van Uffelen, and M. K. Smit, "Upconversion in Er-implanted Al₂O₃ waveguides," *J. Appl. Phys.* **79**(3), 1258–1266 (1996).
13. Purnawirman, E. Hosseini, J. Bradley, J. Sun, G. Leake, T. Adam, D. Coolbaugh, and M. Watts, "CMOS compatible high power erbium doped distributed feedback lasers," in *Advanced Photonics 2013*, H. Chang, V. Tolstikhin, T. Krauss, and M. Watts, eds., OSA Technical Digest (online) (Optical Society of America, 2013), paper IM2A.4.

14. D. L. Veasey, J. M. Gary, J. Amin, and J. A. Aust, "Time-dependent modeling of erbium-doped waveguide lasers in lithium niobate pumped at 980 and 1480 nm," *IEEE J. Quantum Electron.* **33**(10), 1647–1662 (1997).
 15. J. Hoyo, V. Berdejo, T. Toney Fernandez, A. Ferrer, A. Ruiz, J. A. Valles, M. A. Rebolledo, I. Ortega-Feliu, and J. Solis, "Femtosecond laser written 16.5 mm long glass-waveguide amplifier and laser with 5.2 dB cm⁻¹ internal gain at 1534 nm," *Laser Phys. Lett.* **10**(10), 105802 (2013).
-

1. Introduction

Low cost, high performance laser integration technologies that establish power efficient, temperature stable, and large scale multiwavelength on-chip arrays are critical for a variety of important applications including coherent optical communications, integrated analog photonics, microwave signal generation, and high spectral resolution light detection and ranging (LIDAR). A silicon nitride (Si₃N₄) ultra low loss waveguide (ULLW) platform with on-chip propagation losses below 0.1 dB/m [1] and fiber coupling losses of 0.7 dB [1] has demonstrated not only low coupling constant sidewall grating filters with narrow passbands [2], but recently also integrated erbium-doped waveguide distributed feedback (DFB) laser arrays [3].

When compared with semiconductor-based gain media [4–6], rare-earth-ion-doped dielectric gain media, such as erbium-doped aluminum oxide (Al₂O₃:Er³⁺), exhibit relatively narrower lasing linewidths, higher degrees of temperature stability, and lower amplifier noise figures. When reactively co-sputtered onto oxidized silicon wafers Al₂O₃:Er³⁺ has shown relatively low background scattering losses and a broadband, high-gain spectrum for amplification [7]. With the entirety of ULLW platform only requiring a few fabrication steps, the addition of the erbium-doped gain layer by reactive co-sputtering enables streamlined integration of active lasing waveguides with ultra-low loss waveguides and components.

In this letter we report experimental demonstration of both integrated Al₂O₃:Er³⁺ waveguide distributed Bragg reflector (DBR) and distributed feedback lasers on a silicon nitride ultra-low-loss waveguide platform. Record low optical threshold power and high slope efficiency are reported through an optimized cavity design utilizing the highly selective sidewall grating filters enabled by the ULLW platform. Such devices require only a single lithography to define the entirety of the lasing cavity. The distributed Bragg reflector laser designs exhibit pump-to-signal conversion efficiencies up to 5.2% when excited with 974 nm pump light. This is two times greater than that shown by similarly reported devices [8]. Through structural changes to our previously designed DFB lasers [3] we show an improvement of over two orders of magnitude in pump-to-signal conversion efficiency. Spectral traces show emission over a wide wavelength range (1534 to 1570 nm), with side mode suppression ratios (SMSR) of over 50 dB for all designs.

2. Fabrication and lasing structure

Fabrication of the lasing cavities began on 100 mm diameter silicon substrates, upon which 15 μm of thermal oxide (refractive index, n = 1.44) lower cladding was grown. The thickness of the lower cladding ensures that no substrate leakage will occur along the length of the optical path. An 80 nm Si₃N₄ (n = 1.98) lateral guiding layer was deposited by low-pressure chemical vapor deposition (LPCVD), and then subsequently patterned and etched by way of 248 nm stepper lithography and inductively coupled plasma reactive ion etching. The numerical aperture (NA) of the stepper lens, which sets the minimum resolvable feature within the sidewall grating mirrors, also establishes the maximum total die size. Thus, we are constrained to maximum total lasing cavity lengths of no more than 22 mm. A 100 nm thick reactively co-sputtered SiO₂ (n = 1.44) layer, acting as a spacer between the Si₃N₄ core and the Al₂O₃:Er³⁺ active layer (n = 1.65), was then deposited. The devices were then annealed in N₂ at 1050°C for 7h to reduce absorption losses due to Si-H and N-H bonds around 1.52 μm [9]. After annealing, the entire 100 mm wafer was then diced into individual 21 mm x 22 mm die. The 1.67 μm Al₂O₃:Er³⁺ gain layer was then deposited by reactive co-sputtering using a process similar to that reported in [10]. Finally, a mechanical polishing process conditioned

the device facets. The completed cross-section, shown in the left panel of Fig. 1, and the resulting mode profile of the device, shown in the right panel of Fig. 1, are similar to that reported in our previous work [3], albeit now without an oxide top cladding.

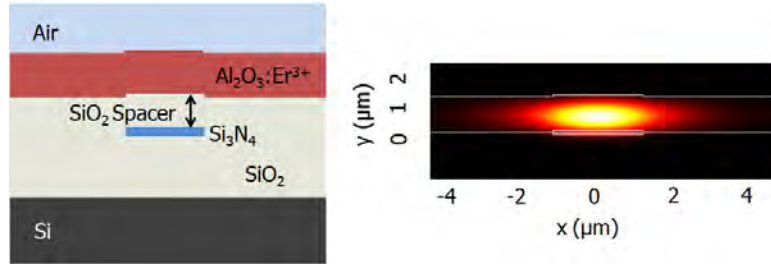


Fig. 1. (Left) Cross-section view of the laser waveguide structure. (Right) Resulting TE-polarized mode profile for laser light operating at 1550 nm.

Through optical backscattering reflectometry measurements [1], we determined the background scattering losses of un-doped reference samples to be below 0.25 dB/cm over the range of 1530-1600 nm. Secondary ion mass spectroscopy measurements quantify the erbium dopant concentration at $1.3 \times 10^{20} \text{ cm}^{-3}$.

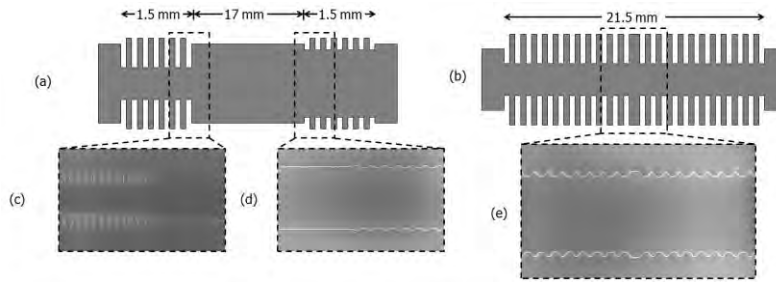


Fig. 2. Top-down schematic images of the Si_3N_4 waveguide DBR (a) and DFB (b) laser cavities. The sidewall grating mirrors are exaggerated to adequately show their detail. Also shown are top-down SEM images of the fabricated Si_3N_4 sidewall grating DBR high reflectivity (c) and low reflectivity (d) mirrors and DFB quarter-wave phase shift section (e). The rounded edges of the fabricated device differ from the intended square-like form of the device design due to a necessary over-exposure of the photoresist during the lithography step.

The DBR resonators consist of straight waveguide sections measuring 17 mm long and $2.8 \mu\text{m}$ wide, with high and low reflectivity mirrors on either end that each measure 1.5 mm long. Figure 2(a) gives a top-down schematic representation of the Si_3N_4 core of the DBR cavity. $250 \mu\text{m}$ and 1.75 mm long \times $2.8 \mu\text{m}$ wide active straight waveguide sections adjacent to the high and low reflectivity mirrors assured adequate space was available between the sidewall grating and the die facet for the mechanical polishing process. The DFB cavities measure 21.5 mm long with $250 \mu\text{m}$ long \times $2.8 \mu\text{m}$ wide active input waveguides on either end between the lasing cavity and the die facet. Figure 2(b) gives a top-down schematic representation of the Si_3N_4 core of the DFB cavity. The pump absorption length of the rare-earth gain material imposes a lower limit on the total device length [11], so to accommodate this constraint our cavity lengths are nearly 3 times longer than the 7.5 mm ones found in our previous designs [3]. Due to the low loss nature of the Si_3N_4 ULLW platform, a serious penalty in overall required lasing gain did not accompany this rather large increase in total device length. Again, the $250 \mu\text{m}$ long active waveguides ensure that sufficient distance between the sidewall grating and the facet is available for polishing. Figures 2(c)-2(e) show scanning electron microscope (SEM) images of the nitride cores of the devices right after the reactive ion etch fabrication step.

Both the DBR and DFB designs used the sidewall grating structure found in [2] to achieve the requisite lasing feedback. Within this configuration periodically varying sections of alternating widths are used to define the grating. It is the width difference between the two waveguide sections that sets the κ parameter, or reflection strength of the grating. For the DBR designs, the high reflectivity mirrors had alternating widths of 1.8 and 3.8 μm , giving a κ value of $\sim 100\text{ cm}^{-1}$. The set with the best performance had low reflectivity mirrors with alternating widths of 2.4 and 3.2 μm , delivering a κ value of $\sim 30\text{ cm}^{-1}$. For the DFB designs, the set with the best performance had alternating widths of 2.55 and 3.05 μm , which in turn produces a κ value of $\sim 16\text{ cm}^{-1}$. The total period length of the sidewall gratings Λ , which sets the lasing wavelength of the devices, was stepped between 478 and 490 nm.

3. Characterization

Figure 3 depicts the experimental setup used to characterize the lasers. Pump light from a 974 nm laser diode is passed through the 980 nm port of a 980/1550 nm wavelength division multiplexer (WDM) and subsequently coupled onto the device die using a 5 μm spot size (at the $1/e^2$ level) lensed fiber. The lasing signal is collected from the device facet and passed through the 1550 nm port of the WDM, after which the output power is quantified using a power meter while the spectrum is recorded by an optical spectrum analyzer (OSA). The coupling loss for the TE-polarized 1550 nm lasing signal and the 974 nm pump laser diode are approximately 6.3 and 5.4 dB, respectively. The device chip was left uncooled throughout the measurements.

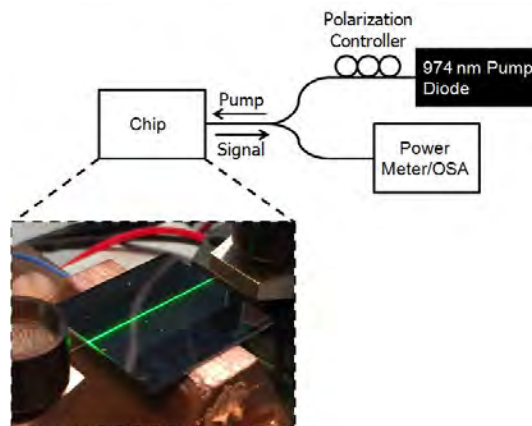


Fig. 3. Measurement setup of the experiment. The inset photo shows the device under 974 nm excitation. For the DBR devices signal light was collected from the side with the low reflectivity mirror. The green emission seen in the waveguide is due to the cooperative upconversion process the erbium atoms experience when under pump excitation [12].

Figure 4(a) shows the single-sided lasing output power as a function of pump laser input power for a DBR operating at 1560 nm (grating period of 486 nm). The lasing threshold is observed at 11 mW of launched pump power, and a maximum on-chip pump power of 55 mW generates an on-chip laser power of 2.1 mW. This corresponds to a pump-to-signal conversion efficiency (η) of 5.2%. Such a low operating threshold and high slope efficiency is a consequence of our strongly reflecting cavity design, as well as the low propagation loss of the LPCVD Si_3N_4 . Figure 4(b) shows the single-sided lasing output power as a function of pump laser input power for a DFB operating at 1546 nm (grating period of 482 nm). Here, the lasing threshold is observed at 21 mW of launched pump power, and for a maximum on-chip pump power of 55 mW we obtain an on-chip laser power of 0.27 mW. This corresponds to a pump-to-signal conversion efficiency of 0.77%, which is a factor of more than 130 times improvement over our design reported in [3]. The main contribution to this improvement in

efficiency came from the extension of the total cavity length from 7.5 mm to 21.5 mm, allowing for sufficient pump light absorption to provide useful lasing gain.

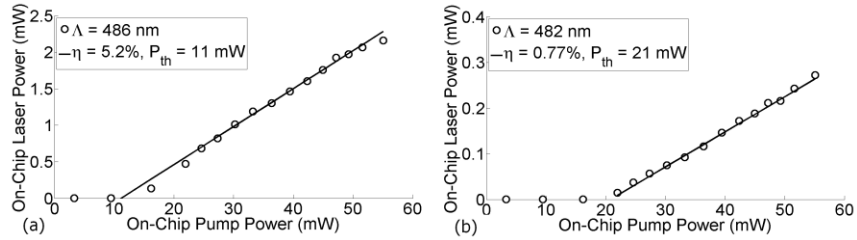


Fig. 4. (a) DBR laser power as a function of launched pump power for the device operating at 1546 nm. (b) DFB laser power as a function of launched pump power for the device operating at 1560 nm.

Figure 5(a) gives the spectra of five different DBR lasers as recorded by the OSA. A simple modification of the grating period within the Si_3N_4 core layer from 478 to 486 nm causes the lasers to output light at 1535, 1541, 1547, 1554, and 1560 nm wavelengths. As is shown, the SMSR for all devices exceeds 50 dB. Figure 5(b) gives the spectra of four different DFB lasers as recorded by the OSA. Here, devices with grating periods between 478 and 490 nm operate at 1534, 1546, 1558, and 1570 nm wavelengths. Again the SMSR for all structures is in excess of 50 dB. The differences in output power seen between the devices can be attributed to differences in the gain threshold and the maximum small signal gain spectrum of the erbium-doped active layer.

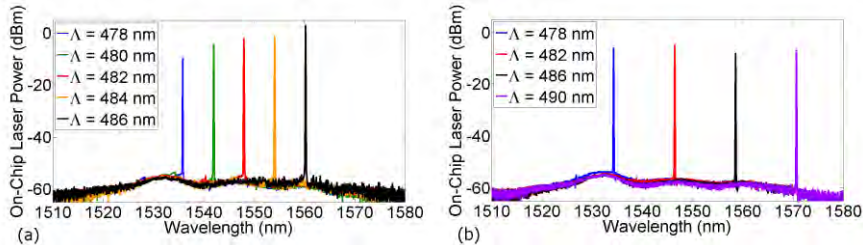


Fig. 5. (a) Superimposed DBR output laser spectra. (b) Superimposed DFB output laser spectra.

Table 1 summarizes the measured performance of all of the DBR and DFB lasers.

Table 1. Measured Performance Parameters of each DBR and DFB Laser

Device Type	Bragg Period (nm)	Lasing Wavelength (nm)	Threshold Power (mW)	Conversion Efficiency (%)
DBR	478	1535	38	0.96
DBR	480	1541	28	1.4
DBR	482	1547	25	2.2
DBR	484	1554	23	2.6
DBR	486	1560	11	5.2
DFB	478	1534	25	0.67
DFB	482	1546	21	0.77
DFB	486	1558	20	0.41
DFB	490	1570	26	0.53

4. Future improvements

When excited under 1480 nm instead of 980 nm light, similar distributed feedback devices [11,13] showed even higher pump-to-signal conversion efficiencies. This difference in performance can mainly be attributed to the long lifetime of the $^4I_{11/2}$ manifold of the erbium ions, resulting in an energy bottleneck when the devices are excited under 980 nm light rather than 1480 nm light [14]. In the future, pumping the devices with 1480 nm instead of 980 nm light would be the best avenue to show immediate improvements in device performance. This would come with an increase in total cost though, as the price per watt is less for 980 nm laser diodes than for 1480 nm diodes. It is this cost constraint that drove the use of a 974 nm pump laser for this work. Another potential avenue for advancement would be to incorporate ytterbium atoms within the Al_2O_3 host material as a sensitizing agent. Such a technique may only make a small improvement though, as efficient energy transfer between the Yb and Er atoms in analogous devices has thus far been limited to host glasses with high phosphorus content [15]. Exciting the distributed Bragg reflector devices from both ends as in [8] and [15] would allow for more on-chip pump light, and thus create a stronger lasing signal, but further levels of device integration could possibly render such an approach impractical. A better solution would be to integrate a sidewall grating filter for the pump light along the output waveguide, as is schematically shown in Fig. 6.

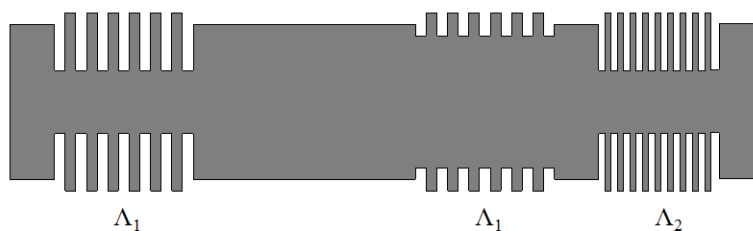


Fig. 6. Top-down schematic of a possible double-pass optical gain DBR structure. Λ_1 and Λ_2 denote the Bragg period for the signal and pump light, respectively.

Such a filter would not only stop the unabsorbed pump light from interfering with subsequent system components down the line, but would also allow for double-pass optical gain. Fabrication of such structures is currently underway.

5. Conclusion

We have experimentally demonstrated erbium-doped waveguide integrated distributed Bragg reflector and distributed feedback lasers on a silicon nitride ultra-low-loss waveguide platform. We demonstrate DBR cavity designs with lasing thresholds of 11 mW and pump-to-signal conversion efficiencies up to 5.2% when excited with 974 nm pump light. For the DFB lasers, structural changes in our lasing cavity design produce an improvement of over two orders of magnitude in pump-to-signal conversion efficiency beyond that found in our previous work. Spectral traces show emission over a wide wavelength range (1534 to 1570 nm), with SMSRs of over 50 dB for all designs. Development of a suitable active-to-passive transition region would allow for complete integration of these lasers within the ULLW platform and work towards such an endeavor is currently underway.

Acknowledgments

The authors thank Michael L. Davenport and Taran Huffman for their insights. This work was supported by DARPA MTO under the iPhoD (grant no. HR0011-09-C-0123) and EPHI (grant no. HR0011-12-C-0006) contracts. The views and conclusions contained in this document are those of the authors and should not be interpreted as representing official policies of the Defense Advanced Research Projects Agency or the U.S. Government.